Water Resources Research

RESEARCH ARTICLE
10.1029/2021WR030881

Unprecedented High Northern Australian Streamflow Linked to an Intensification of the Indo-Australian Monsoon

P. A. Higgins[1,2], J. G. Palmer[2,3,4], M. P. Rao[5,6,7], M. S. Andersen[8], C. S. M. Turney[2,3,4,9], and F. Johnson[1]

[1]Water Research Centre, School of Civil and Environmental Engineering, University of New South Wales, Sydney, NSW, Australia, [2]ARC Centre of Excellence in Australian Biodiversity and Heritage, University of New South Wales, Sydney, NSW, Australia, [3]Chronos [14]Carbon-Cycle Facility, Mark Wainwright Analytical Centre, University of New South Wales, Sydney, NSW, Australia, [4]Earth and Sustainability Science Research Centre, School of Biological, Earth and Environmental Sciences, University of New South Wales, Sydney, NSW, Australia, [5]Cooperative Programs for the Advancement of Earth System Science, University Corporation for Atmospheric Research, Boulder, CO, USA, [6]Department of Plant Science, University of California, Oakland, CA, USA, [7]Tree-ring Laboratory, Lamont-Doherty Earth Observatory of Columbia University, Palisades, NY, USA, [8]Water Research Laboratory, School of Civil and Environmental Engineering, University of New South Wales, Sydney, NSW, Australia, [9]Now at Division of the Deputy Vice-Chancellor, Research, University of Technology, Sydney, NSW, Australia

Key Points:

- 592-year annual streamflow reconstruction of the Daly River Catchment, Australia, derived using a tree-ring network
- Wavelet-based techniques to transform tree ring spectral characteristics improve the reconstruction ability
- High streamflow in the twentieth Century is regionally coherent and unprecedented in the preceding five centuries

Supporting Information:

Supporting Information may be found in the online version of this article.

Correspondence to:

P. A. Higgins,
philippa.higgins@unsw.edu.au

Citation:

Higgins, P. A., Palmer, J. G., Rao, M. P., Andersen, M. S., Turney, C. S. M., & Johnson, F. (2022). Unprecedented high Northern Australian streamflow linked to an intensification of the Indo-Australian monsoon. *Water Resources Research*, *58*, e2021WR030881. https://doi.org/10.1029/2021WR030881

Received 26 JUL 2021
Accepted 3 FEB 2022

Author Contributions:

Conceptualization: P. A. Higgins
Data curation: P. A. Higgins, J. G. Palmer
Formal analysis: P. A. Higgins
Methodology: P. A. Higgins, J. G. Palmer
Software: M. P. Rao
Supervision: M. S. Andersen, C. S. M. Turney, F. Johnson
Visualization: P. A. Higgins
Writing – original draft: P. A. Higgins
Writing – review & editing: J. G. Palmer, M. P. Rao, M. S. Andersen, C. S. M. Turney, F. Johnson

Abstract Streamflow in Australia's northern rivers has been steadily increasing since the 1970s, most likely due to increased intensity in the Indo-Australian monsoon. However, because of limited data availability, it is hard to assess this recent trend and therefore contextualize potential future climatic changes. In this study, we used a network of 63 precipitation-sensitive tree-ring chronologies from the Indo-Australian and Asian monsoon regions to reconstruct streamflow in the Daly catchment in the Northern Territory of Australia from 1413 to 2005 CE. We used a novel wavelet-based method to transform the variance structure of the tree-ring chronologies to better match the hydroclimate prior to reconstruction with a hierarchical Bayesian regression model. Our streamflow reconstruction accounts for 72%–78% of the variance in the instrumental period and closely matches both historical flood events and independent proxy records, increasing confidence in its validity. We find that while streamflow has been increasing since the 1800s, the most recent 40-year period is unprecedented in the last ~600 years. Comparison to an independent coral-based streamflow record shows regional coherency in this trend. Extreme high flows were found to be linked to La Niña events, but we found no significant relationship between streamflow and El Niño events, or streamflow and other regional climatic drivers. More work is therefore needed to understand the drivers of the recent streamflow increase, but, regardless of the cause, water managers should be aware of the paleoclimatic context before making decisions on water allocations.

Plain Language Summary Large-scale agricultural development has been proposed for the Daly catchment in the Northern Territory of Australia. Since the start of record keeping in the Daly catchment in the 1970s, streamflow has been steadily increasing, most likely due to increases in Australian monsoon rainfall. However, because of the limited amount of data, it is hard to assess whether this recent increase in streamflow is unusual, part of a longer trend, or a natural cycle in monsoon rainfall. In this study, we used rainfall-sensitive tree growth and a statistical model to reconstruct Daly River streamflow over the past 592 years. Our streamflow reconstruction closely matches known past flood events, increasing confidence in its validity. We find that streamflow has increased since the 1800s but that the most recent 40-year period is unprecedented in the last 600 years. More work is needed to understand the drivers of this increased streamflow but regardless of the cause, water managers should be aware of the Daly River's history before making decisions on allocating water to agriculture or other large users.

1. Introduction

Water resources in the large floodplains of monsoonal north Australia are determined by the onset, duration, and intensity of the Indo-Australian summer monsoon (IASM). Importantly, recharge to aquifers contributing critical dry season discharge to groundwater fed springs and rivers is also linked to the intensity of monsoon rainfall (McCallum et al., 2010; Singh et al., 2019). Endemic flora and fauna, and the cultural values of Indigenous

peoples, are dependent on the wet/dry seasonality in flows (CSIRO, 2009; Russell-Smith et al., 1997). The IASM is closely tied to the El Niño–Southern Oscillation (ENSO). Both climatic phenomena, the IASM and ENSO, exhibit substantial inter-annual and decadal variability (Smith et al., 2008; Suppiah, 1992). This variability can cause both droughts and floods, with severe impacts on the lives and livelihoods of people living in the region.

Since 1950, monsoonal Australia has experienced an increase in summer rainfall (Taschetto & England, 2009), and annual streamflow (Zhang et al., 2016), thought to be a result of changes in the IASM. Historical meteorological records from ship logs show that this recent trend is part of a longer-term intensification of the IASM, occurring at least since the early 1800s (Gallego et al., 2017). Despite this intensification, rainfall variability remains high; consecutive years of monsoon failure occurred during the 2018–2019 and 2019–2020 wet seasons, resulting in very low river levels and water restrictions over much of Australia's north (BOM, 2019, 2020).

It is highly uncertain whether the recent trend in rainfall will continue. Projections of future monsoon rainfall are challenging because of the strong climate coupling between the land, atmosphere, and oceans. Climate models predict a future thermodynamic increase in mean monsoonal rainfall (Christensen et al., 2013), however, there are large inter-model uncertainties, most notably for the IASM (Brown et al., 2017). The ensemble mean of the Climate Model Intercomparison Project Phase 5 projects an increase in IASM rainfall variability at daily to decadal timescales (Brown et al., 2017). Increased variability has important implications for the management of water resources, as existing infrastructure, management plans, and entitlements may be inadequate for future changes (De Loe & Kreutzwiser, 2000), particularly in regions like monsoonal Australia where water storage potential is limited (CSIRO, 2009).

Palaeohydrological reconstructions are useful tools for supporting water resource management and planning under uncertainty (Allen et al., 2015; Rice et al., 2009). There has been a recent interest in palaeohydrological reconstructions for monsoon rivers (e.g., Nguyen et al., 2020 and references therein) due to the inability of short instrumental records to fully characterize hydroclimatic variability, and uncertainty around future changes in streamflow and flood frequency (Rao et al., 2020). Long reconstructed records can increase our understanding of variability in monsoon streamflow and floodplain dynamics, as well as their relationship with major drivers of climate variability such as ENSO. However, very few streamflow reconstructions are available for the IASM region (see D'Arrigo et al., 2011; Verdon-Kidd et al., 2017) in part due to the limited availability of high-resolution (sub-annual to annual) precipitation and streamflow proxies across the region (Allen et al., 2015; D'Arrigo et al., 2008). There is an urgent need for multi-centennial reconstructions of streamflow variability in monsoonal Australia to reduce the uncertainty over the impact of future climate change and increasing resource demands.

The Daly River, a monsoonal river system in the northwest of the Northern Territory, is one of the northern Australia's largest rivers and one of the few with perennial flows (Morrison, 1970). Annual streamflow is highly dominated by monsoon rainfall, with dry season flows, fed by groundwater discharge, accounting for less than 10% of total annual flow. Reliable stream gauging stations and monitoring bores for the Daly River system are sparse. Very limited data exists prior to the mid-1970s and there is low confidence in dry season flow records for many gauges. The paucity of data greatly inhibits the potential to assess the linkages between the hydrological regime, resource availability and dependent ecosystems (CSIRO, 2009). Declining rainfall trends in southern Australia and the perception of abundant land and water resources in the monsoon tropics have recently renewed interest in agricultural development in northern Australia and the Daly region (Petheram et al., 2008; Yeates et al., 2013). With limited storage potential in seasonally dynamic aquifers, increased dry season agricultural demand is likely to change surface and groundwater regimes with consequences for the environment (CSIRO, 2009). Extending short hydrological records is essential for improving the assessment and management of water resources in the Daly catchment and the IASM region more broadly.

Here we present a paleohydrologic reconstruction of Daly River streamflow that extends available instrumental observations by more than five centuries and discuss its linkages with both changes in the IASM and Pacific atmosphere-ocean climate variability. Our Daly River streamflow reconstruction was developed using a tree-ring network from across the IASM region and remote sites with strong teleconnections to the IASM. We demonstrate the benefits of a new method for paleohydrologic reconstruction, in which a wavelet-based variance transform maximizes the ability of the tree-ring predictors to characterize the hydroclimate, resulting in a streamflow reconstruction that better matches the instrumental data. We then compare our record to other observational and proxy records for the region, specifically low-resolution sediment cores from the Daly River and a coral-based river

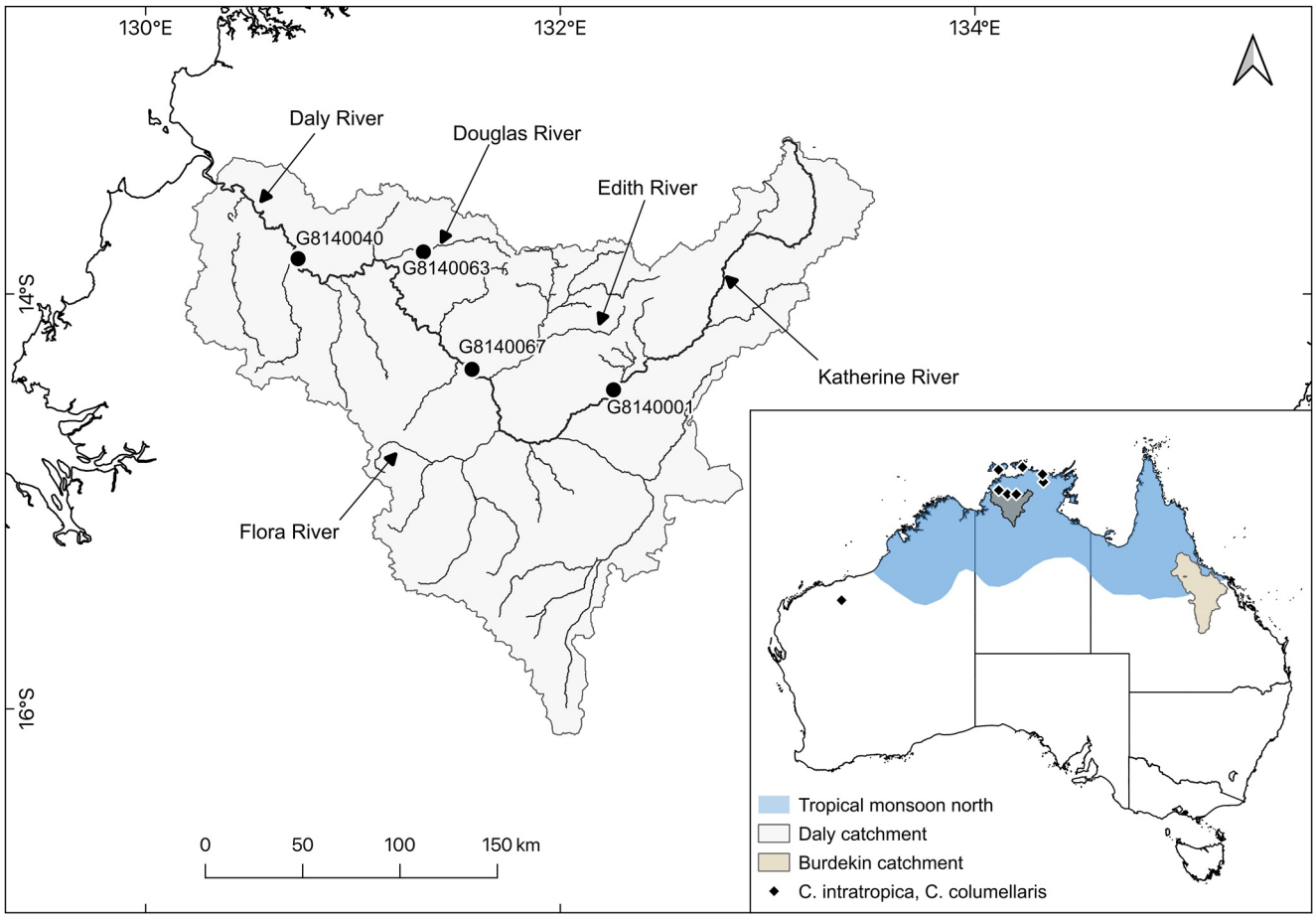

Figure 1. The Daly catchment showing the location of the four selected stream gauges (black circles with gauge numbers). The inset map shows the location of the Daly catchment (gray) and Burdekin catchment (beige) within the Australian tropical monsoon region (light blue), and the locations of *Callitris intratropica* and *C. columellaris* tree-ring chronologies within and proximal to the monsoon region (black diamonds). The approximate southern monsoon region boundary was adapted from the Australian Bureau of Meteorology climate classification.

reconstruction from subtropical eastern Australia, demonstrating that recent increases in streamflow are regionally coherent and unprecedented in the reconstruction interval.

2. Study Area and Data Availability

2.1. The Daly Catchment

The 320-km Daly River flows from the foothills of Arnhem Land to discharge into the Timor Sea in the northwest, with a catchment area of approximately 53,000 km^2 (Figure 1). Important tributaries of the Daly River include the Katherine, which contributes around 40% of the total flow in the system, and the Flora, Edith and Douglas rivers, all of which have high conservation and tourism value (CSIRO, 2009)

The Daly region receives an average of 1,020 mm of rainfall annually of which more than 95% falls in the November to April wet season. Annual potential evapotranspiration is 1,940 mm/year; thus the region is water limited (CSIRO, 2009). There is a steadily increasing trend in total annual rainfall (significant at $p < 0.001$; Mann–Kendall test) throughout the historical period (Figure 2a) and consequently, evapotranspiration is also increasing due to increased catchment water availability (Wasko et al., 2021). Annual streamflow is closely linked to wet season rainfall, with an average of 94% of runoff occurring during wet season months. Peak discharge occurs during January, February, and March (Figure 2b). Dry season baseflow in the perennial reaches of the Katherine and Daly rivers is the result of discharge from the region's two major karstic aquifers, the Tindall Limestone and

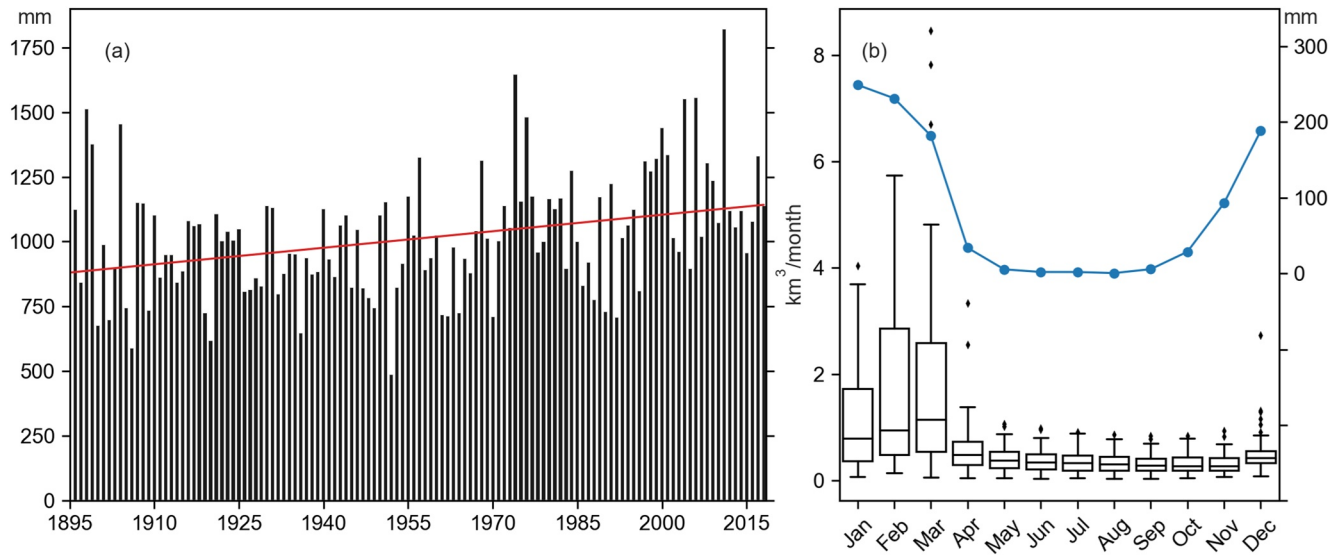

Figure 2. (a) Catchment average annual water year (September–August) rainfall (mm) from 1896 to 2018, with the long-term trend shown in red; (b) Boxplots showing monthly discharge (km^3/month, left axis) for the instrumental period (1961–2018) at gauge G8140040, Daly River at Mount Nancar, with catchment average monthly rainfall (mm, right axis) plotted in blue.

the Oolloo Dolostone (CSIRO, 2009). Variations in dry season baseflow are due to higher or lower aquifer levels in the preceding wet season (CSIRO, 2009).

2.2. Hydrological Data

Daily streamflow data (ML/day) for gauges in the Daly River catchment were downloaded from the Northern Territory Government Water Data Portal at https://water.nt.gov.au/. Gauges on perennial rivers with at least 40 years of data before 2005 (the last year for many tree-ring chronologies) were selected. Suitable gauges were identified on the Douglas River downstream of the Old Douglas Homestead, the Katherine River at Railway Bridge, and the Daly River upstream of Dorisvale Crossing (Figure 1). For the Daly River at Mount Nancar, the gauge nearest to the catchment outlet, the time series was extended from 1961 to 1971 using data from nearby gauges and a regression model (see Supporting Information S1).

Years with more than 15% of daily values missing during the peak discharge period (January–March), were excluded from analysis (Table 1). For other years, gap-filled daily streamflow data was downloaded from the Australian Bureau of Meteorology (BOM) Hydrologic Reference Stations database (http://www.bom.gov.au/water/hrs/index.shtml). Annual streamflow (km^3) was then calculated for the Northern Territory water year of September to August (CSIRO, 2009). Streamflow between the four gauges is highly correlated (Pearson $r = 0.78$–0.97; Figure S2 in Supporting Information S1). Including all four gauges in the reconstruction model meant that 1962 was the only year without any streamflow data (i.e., missing data from all four gauges).

Table 1
Selected Streamflow Gauges in the Daly Catchment

Gauge number	River	Gauge location	Catchment area (km^2)	Average annual flow (km^3)	Data period	Missing years (before 2005)
G8140040	Daly	Mount Nancar	47,652	8.55	1961–2018	1962, 1966, 1977, 1978, 1985
G8140067	Daly	Upstream Dorisvale Crossing	33,227	5.79	1966–2018	1968, 1975, 1980, 1989, 1991, 2000
G8140063	Douglas	Old Douglas Homestead	831	0.25	1959–2018	1962, 1968, 1969, 1971, 1976, 1977, 1993, 2002
G8140001	Katherine	Railway Bridge	8,357	2.34	1963–2018	1971, 1975

Daly catchment-average water year rainfall was calculated from monthly gridded data from the Queensland Government SILO Climate Database (https://www.data.qld.gov.au/dataset/silo-climate-database). Daily rainfall for the town of Katherine was downloaded for the BOM gauges 014,902 and 014,903 from their website at http://www.bom.gov.au/climate/data/. Years missing more than 15% of daily rainfall values were excluded from the analysis. The Global Precipitation Climatology Project (GPCP; Adler et al., 2003) monthly gridded rainfall from 1979 to 2020, used to calculate the correlation between Daly catchment and regional rainfall, and the Extended Reconstructed Sea Surface Temperature (ERSST) v5 dataset Huang et al. (2017), were both obtained from the NOAA/OAR/ESRL PSL website at https://psl.noaa.gov/.

2.3. Historical Flood Records

The largest settlement in the Daly catchment is the town of Katherine on the Katherine River, also the location of gauge G8140001. Three significant flood events, in 1998, 2006, and 2011, have occurred since streamflow was reliably recorded at Katherine. However, only the 1998 event falls within the reconstruction period. Pre-instrumental data sources, predominantly newspaper articles, provide a record of major flood events since the permanent European occupation of the region began in 1872. Large floods at Katherine occurred in December 1897 (reconstruction year 1898), 1914, 1931, 1940, and 1957 (Water Studies Pty Ltd., 2000).

2.4. Tree-Ring Proxy Records

Very few tree-ring chronologies exist for the tropics, including northern Australia, due to the difficulty in finding tropical tree species with annual growth rings (Rozendaal & Zuidema, 2011). However, recent efforts have identified the dendrochronological potential of both *Callitris intratropica* and *C. columellaris* (cypress pine) species (Allen et al., 2019, 2020; Baker et al., 2008; O'Donnell et al., 2015). While these species have great potential to inform understanding of the hydroclimate of monsoonal Australia (Allen et al., 2020; D'Arrigo et al., 2008), the chronologies developed to date are short, with the majority ∼100–250 years in length. Longer reconstructions can be developed by utilizing remote tree-ring proxies (Allen et al., 2015) from regions with strong teleconnections to monsoonal Australia. For the initial predictor pool, we downloaded all publicly available tree-ring chronologies from Australia, New Zealand and Monsoonal Asia located between 70°E, 40°N and 180°E, 47°S (Figure S4 in Supporting Information S1) from the International Tree Ring Databank (ITRDB). The wood property series from each site were converted to chronologies by the process of standardization (i.e., detrended and transformed into dimensionless growth indices). The process aims to remove growth trends thought to be largely unrelated to climate using the "signal free" (Melvin & Briffa, 2008) and "Regional Curve Standardization" (Briffa et al., 1992) methods of tree-ring standardization.

3. Methods

Figure 3 provides a schematic overview of the methods used to reconstruct Daly catchment streamflow. The methods are described briefly below and in further detail in the Supporting Information S1.

3.1. Streamflow Reconstruction

Tree rings are useful predictors of streamflow because both tree growth and variations in streamflow are controlled by soil moisture, which is influenced by rainfall and evapotranspiration (Meko et al., 1995). However, tree rings provide only indirect information about climate variations. In addition, factors including local proxy noise, seasonal sensitivities, and standardization methods result in biases in the high-to low-frequency spectrum of proxy records compared to the instrumental datasets they are attempting to reconstruct (Franke et al., 2013). Spectral biases are likely to be compounded when using remote tree-ring chronologies in reconstructions as only a portion of the climatic information contained in the proxy—related to the teleconnection—is relevant to the reconstruction.

To address these issues, after selecting the tree-ring chronology predictor pool, we applied a novel method for paleohydrologic reconstruction, in which a unique wavelet-based variance transform (Jiang et al., 2020, 2021) was used to modify the spectral characteristics of each tree-ring chronology to better match Daly catchment average annual rainfall (see Supporting Information S1). A nested hierarchical Bayesian regression model with

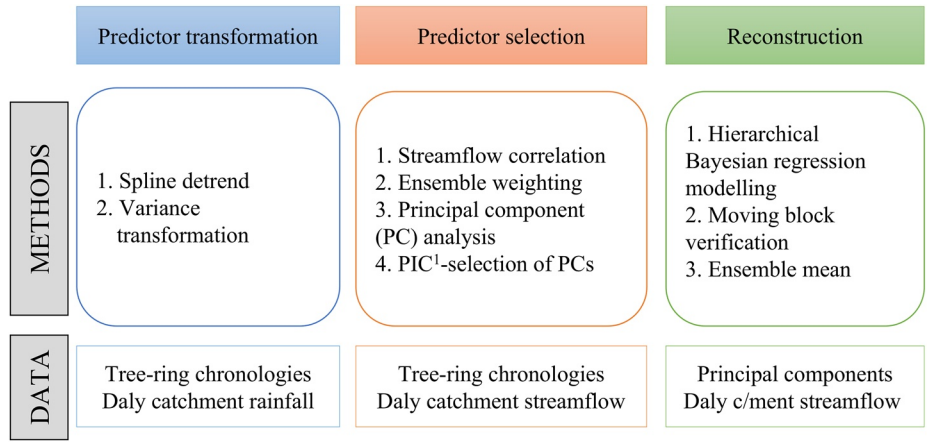

Figure 3. Schematic overview of the reconstruction methodology. [1]Partial information correlation.

partial pooling (Devineni et al., 2013; Rao et al., 2018), which is suitable for our short data records with missing years, was then used to produce the streamflow reconstruction from the transformed chronologies. The partial pooling framework combines the regression strength of the model across the four gauges, which can result in lower uncertainty in estimated parameters and reconstructed discharge, as well as improved final model skill (see Supporting Information S1). We used a moving block calibration-verification scheme (Nguyen et al., 2020) in which 7-year, overlapping periods of the instrumental record were successively withheld to independently test the modeling (see Supporting Information S1).

To evaluate the reconstruction, we used standard verification tests in dendrochronology: the calibration period coefficient of multiple determination (CRSQ or R^2), the validation period reduction of error (VRE), and the validation period coefficient of efficiency (VCE; Cook & Kairiukstis, 1990). The VCE is equivalent to the Nash-Sutcliffe efficiency test (Nash & Sutcliffe, 1970) and is the most stringent verification criteria. The Bayesian R^2, a data-based estimate of the proportion of the variance explained for new data Gelman et al. (2019), and the Sign Test, which calculates the number of years that the reconstruction correctly (+) or incorrectly (−) tracks the sign of observations during the calibration period (Cook & Kairiukstis, 1990), were also used in verifying the model.

3.2. Historical Flood Events

To further verify our results, the ability of the streamflow reconstruction to identify historical flood events recorded at the Katherine township was assessed via superposed epoch analysis (SEA), a compositing technique that tests the probability of an association between high flows and flood years occurring by chance (Haurwitz & Brier, 1981; Rao et al., 2019). To apply SEA to flood identification in our reconstruction, the six historical flood events which occurred during the reconstruction interval were used as key event years for SEA. A composite matrix was created by selecting reconstructed streamflow at Katherine (G8140001) from 10 years prior to 5 years following each event. Streamflow was normalized to the 10 years before an event to remove noise unrelated to the event signal, then averaged across all events to determine the composite signal (see Supporting Information S1). The significance of the flood event-streamflow relationship was tested by comparing the key event composite to that generated from 10,000 draws of 6 years at random without replacement ("pseudo-flood years") from the reconstruction between 1888 (first event year—10) and 2005 CE.

3.3. Extreme Event Analysis and Climate Forcing

Extreme dry/wet events were classified as those exceeding below the 5th and above the 95th percentiles of flows, respectively, during the reconstruction period (1413–2005 CE). Changes in the frequency of extreme events were estimated using a nonparametric Gaussian kernel function (Mudelsee et al., 2004) with bandwidth selected via the method of Sheather and Jones (1991) and 95% confidence intervals estimated based on 1,000 bootstrap simulations. Trends in the recurrence rate of extreme events were tested against the null hypothesis of constant recurrence rate using the Cox-Lewis statistic (Cox & Lewis, 1966):

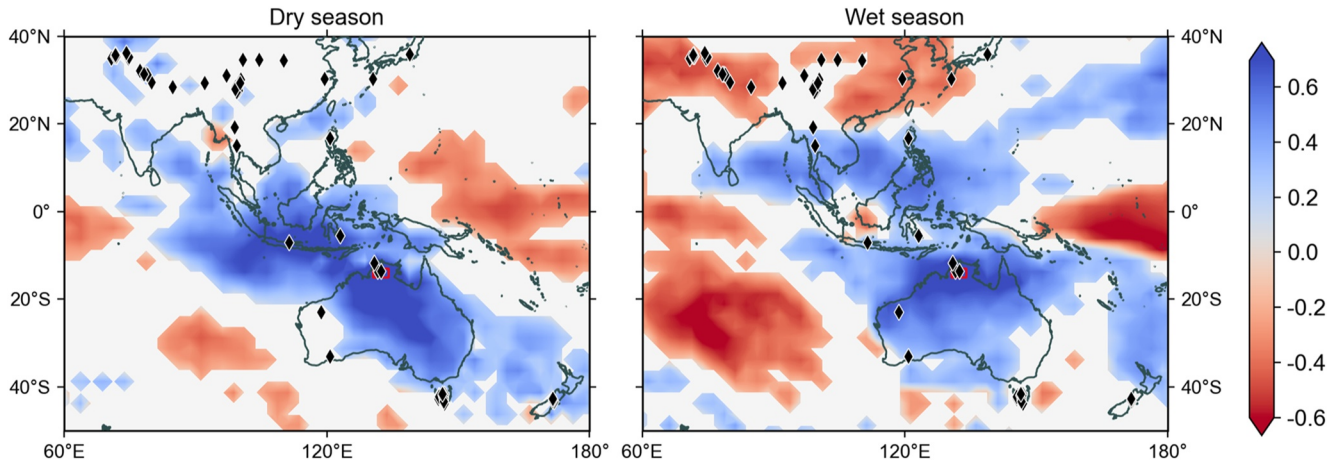

Figure 4. Left: Spatial Pearson correlation fields comparing average Daly catchment (red square) the Global Precipitation Climatology Project (GPCP) rainfall and GPCP rainfall over Australia, the South-east Asian Monsoon and Asian Monsoon regions during the northern Australia dry season (May–September) between 1979 and 2020. Right: Same figure for the northern Australia wet season (November–April). Correlations not significant at $p < 0.1$ are greyed out. Black diamonds represent the location of the 63 tree-ring chronologies with a significant correlation to at least three of four Daly catchment streamflow gauges after variance transformation.

$$U = \frac{\sum_{j=1}^{m}(T_{event}(j)/m) - [T(1) + T(n)]/2}{[T(n) - T(1)] \times (12m)^{-1/2}}$$

which is a standard normal distribution under the null hypothesis (Mudelsee et al., 2003), where $T(1)$, $T(n)$ are the first and last years of the observation interval, and m is the number of extreme events.

Bootstrapping was used to assess whether extreme events are significantly associated with different ENSO phases (Allen et al., 2020). The occurrences of El Niño/La Niña events since 1875 were determined based on December–February (DJF) Nino3.4 sea surface temperature (SST) anomalies above/below 0.5°C and referenced against the events listed on the Australian Bureau of Meteorology website (www.bom.gov.au). Bootstrap replicates were drawn with replacement from the SST data to match the same number of years as the wet and dry extremes. The co-occurrence of extremes and ENSO phases was considered significant if the number of actual events lay outside the 95% bias-corrected and accelerated (BCA) bootstrap confidence interval (Efron, 1987) of the distribution based on 30,000 bootstrap replicates. The number of bootstrap replicates was increased from 1,000 until the confidence interval remained unchanged.

4. Results and Discussion

4.1. Tree-Ring Predictor Selection

Figure 4 shows the correlations between Daly catchment average rainfall and rainfall from regions with strong teleconnections to the IASM, during both the dry and wet (monsoon) seasons. Daly catchment rainfall is significantly correlated to rainfall in southeastern Australia during the May–September dry season when Indian Ocean sea surface temperatures affect Australian rainfall (McBride & Nicholls, 1983; Risbey et al., 2009). Conversely, Daly catchment rainfall is significantly anti-correlated to the Asia Summer Monsoon during the November-April wet season, reflecting coherence between the regional monsoons (Wang et al., 2014). Correlations between Indonesian and northern Australian rainfall are significant throughout the year but are stronger during the dry season.

Figure 4 also shows the locations of the 63 tree-ring chronologies with significant correlation to Daly catchment streamflow retained for the final model (see Table S1 in Supporting Information S1 for details). Nearly 70% of the retained predictors are from regions impacted by monsoon rainfall. Five chronologies are within the IASM region, of which three are proximal to the Daly catchment (within 20 km, see Figure 1). A further 36 are within the Asian Summer Monsoon region, and the remaining 22 from subtropical to temperate Australia, and New Zealand.

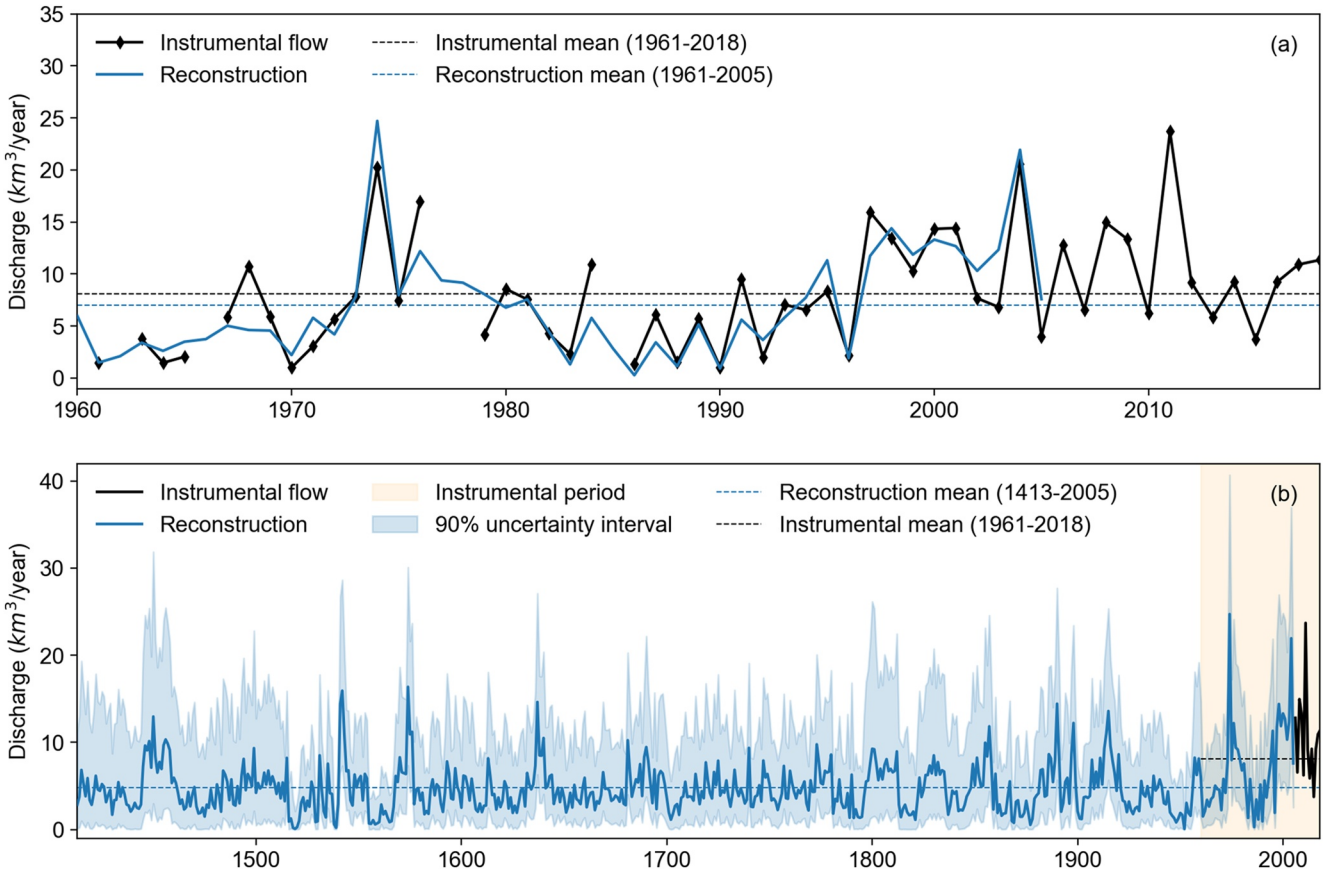

Figure 5. (a) Instrumental (black) versus reconstructed (blue) streamflow in km^3/year for Daly River gauge G8140040 over the instrumental period 1961–2018. (b) Reconstructed flow at G8140040 from 1413 to 2005 CE with the 90% confidence interval for the reconstruction shown in light blue.

Absolute Pearson correlations between streamflow and significant tree-ring predictors vary from $r = 0.28$ to 0.61 with a median value of $r = 0.42$. This is a substantial increase in correlation compared to the pre-transform predictors, which varies from $r = 0.0$ to 0.51 with a median value of $r = 0.21$. Transforming the spectral variance of the tree-ring chronologies is therefore shown to strengthen their correlation to Daly catchment streamflow.

4.2. Streamflow Reconstruction

The final nested reconstruction based on the variance transformed tree-ring chronologies spans 1413 to 2018 CE, with instrumental data appended after 2005. Figure 5a compares observations with reconstructed streamflow at the most downstream gauge, G8140040 at Mount Nancar, using the tree-ring data for the best replicated (1898–2005) nest. Results for the other three gauges are shown in Figure S9 in Supporting Information S1. This reconstruction accounts for 72%–78% of the variance in streamflow observations at each gauge over the calibration period from 1959 to 2005. Table 2 shows the calibration-validation statistics used to evaluate the validity and stability of the nested models for the best-replicated nest, and median statistics of all nests between 1413 and 2005 CE. Timeseries results for all nests are provided in Figure S10 in Supporting Information S1.

The calibration and verification statistics demonstrate that the reconstruction is reliable, despite the relatively short calibration period. Despite the decreasing number of tree-ring predictors moving back in time, the statistical results remain strong for the earliest part of the record, with the least replicated nest accounting for 59%–62% of the calibration period variance. Uncertainty intervals (Figure S9 in Supporting Information S1) show that the fifth percentile VRE and VCE values are above zero throughout the reconstruction period, indicating that the reconstruction contains meaningful information over its entire length (Cook & Kairiukstis, 1990). In addition, the significant ($p < 0.01$) Sign Test results are a good indication that the tree-ring chronologies are accurately tracking the direction of year-on-year variability in streamflow during the calibration period.

Table 2
Calibration and Verification Statistics for the Best-Replicated Nest (1898–2005) and Median Values for the Whole Reconstruction Interval (1413–2005) for the Four Daly Catchment Gauges

	Initial nest (1898–2005)					Median values (1413–2005)			
Gauge number	R^2	Bayes R^2	VRE	VCE	Sign test (p)[a]	R^2	Bayes R^2	VRE	VCE
G8140040	0.78	0.62	0.60	0.36	27 + 8 − (0.002)	0.68	0.58	0.61	0.36
G8140067	0.78	0.65	0.59	0.34	23 + 4 − (<0.001)	0.69	0.58	0.61	0.40
G8140063	0.78	0.64	0.69	0.50	27 + 5 − (<0.001)	0.70	0.59	0.66	0.37
G8140001	0.72	0.60	0.56	0.26	28 + 6 − (<0.001)	0.67	0.57	0.57	0.26

[a]*n is* less than the number of calibration years due to data gaps.

The full reconstruction for G8140040 is shown in Figure 5b; results are similar for the other gauges (not shown). The reconstruction shows that streamflow during the instrumental period represents a period of unusually high flow that is unprecedented in the preceding five centuries. The 57-year gauge instrumental period from 1961 to 2018 has mean streamflow of 7.79 km^3/year, which is significantly higher ($p < 0.001$, two-sided Student's t-test) than the pre-instrumental mean of 4.60 km^3/year, and any period of equivalent length in the reconstruction. Similarly, the gauge calibration period from 1961 to 2005, which has mean streamflow of 6.99 km^3/year, exceeds any previous 44-year period, but the difference is not significant for periods between 1873 and 1922 CE. These results are consistent with an intensification of IASM rainfall starting in the early to mid-1800s.

4.3. Historical Comparisons

The largest recorded flood event at Katherine occurred in 1998 after ex-Tropical Cyclone Les brought 400–500 mm of rain within three days (Skertchly & Skertchly, 1999). The rainfall characteristics of other major historical flood events are similar, with several hundred millimeters of rain falling within a few days (Water Studies Pty Ltd., 2000). There is a moderately strong and significant positive correlation ($r = 0.60$; $p < 0.001$) between the annual maximum 5-day rainfall, which represents the approximate length of rainfall events resulting in historical floods, and total water year rainfall at Katherine (Figure 6). In most cases, major floods occurred during very wet years, with total rainfall in the top ~11% of the record. The exceptions are 1914 and 1931, which were average rainfall years. These results are indicative only as extreme rainfall events, especially those related

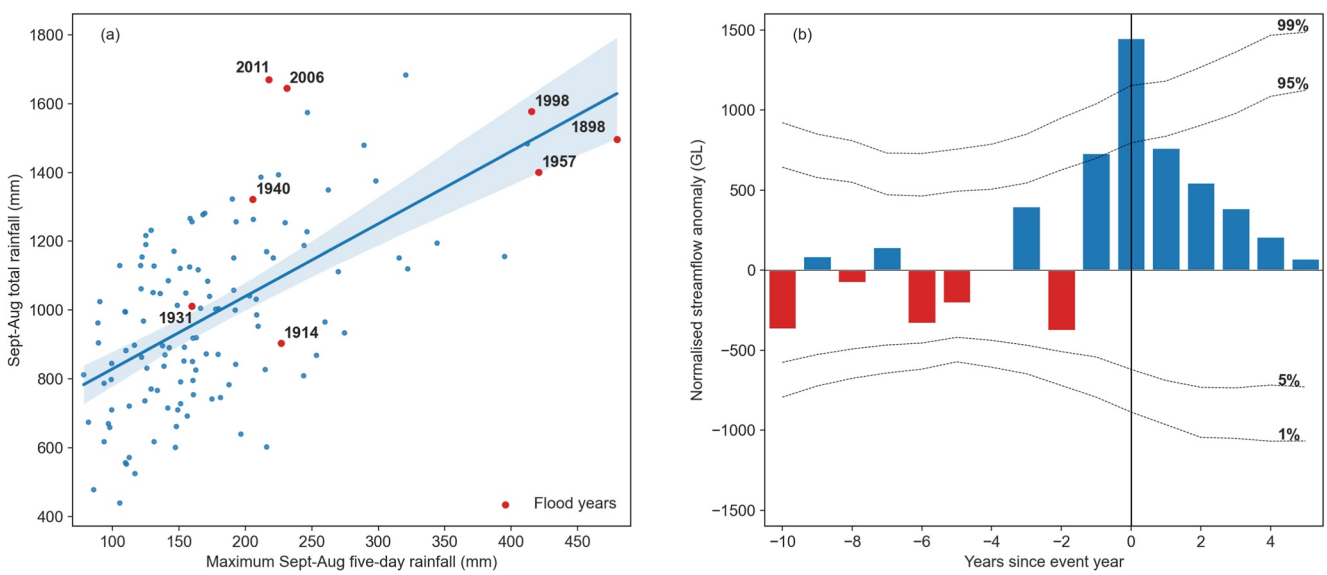

Figure 6. (a) Relationship between maximum 5-day rainfall and total annual (September–August) rainfall at Katherine for all years on record (blue) and historical flood years (red). The blue line shows the significant positive trend ($r = 0.60$; $p < 0.001$) between the variables within the 95% confidence interval. (b) Superposed epoch analysis showing that Katherine River streamflow is significantly ($p < 0.01$) higher than expected by chance during historical flood years.

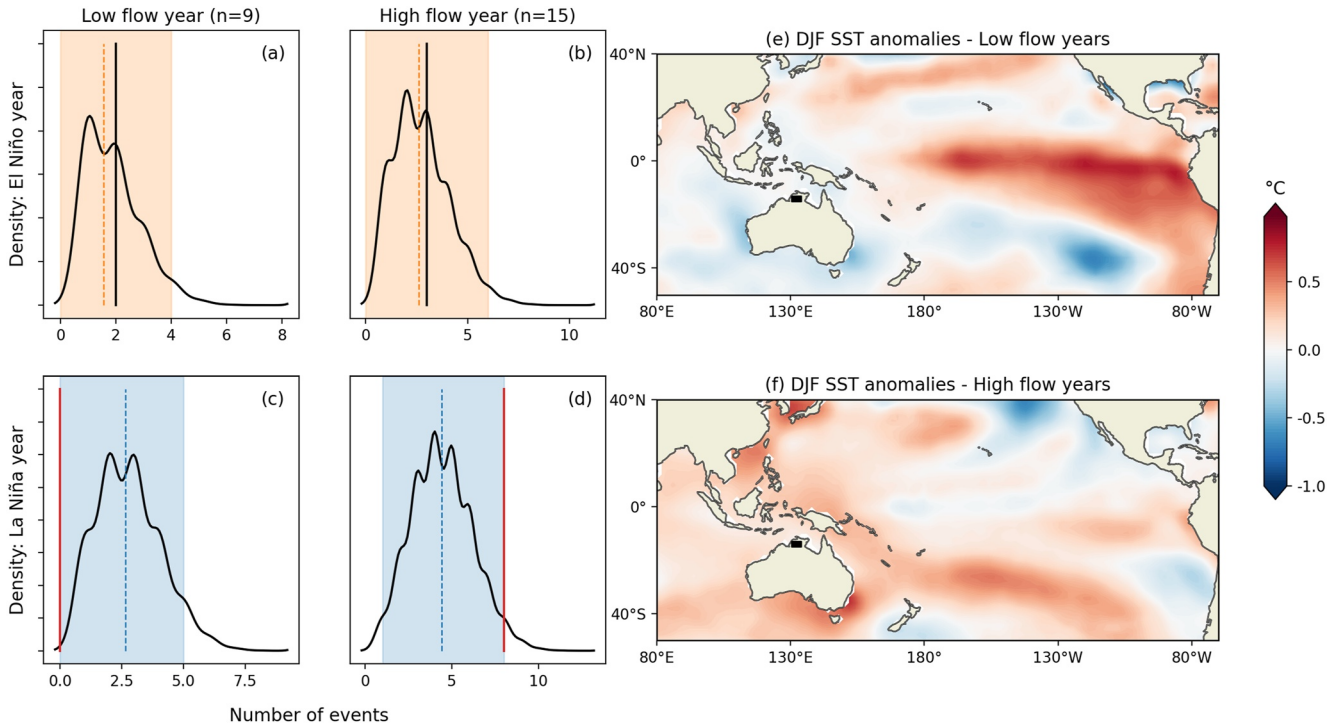

Figure 7. Kernel density estimate plots of 30,000 bootstrapped replications of instrumental Nino3.4 DJF SST anomalies from 1875 to 2005 showing the co-occurrence of extremes in the reconstructed streamflow and El Niño (a), (b) and La Niña (c), (d) events. The number of extreme low and high flow events in the reconstruction associated with each ENSO phase is shown in black and compared to the bootstrap mean (dashed lines); significant values lying outside the 95% bias-corrected bootstrap confidence interval are shown in red. The average December to January (DJF) SST anomalies during low flow years (e) and high flow years (f) are also shown, with the approximate location of the Daly catchment indicated by the black square.

to cyclonic rainfall, are not evenly distributed over the catchment, and there is a paucity of rainfall gauges in the early part of the record.

The significant positive relationship between high-intensity events which may cause flooding and total annual rainfall suggests flood years should be identifiable by higher-than-average reconstructed Katherine River streamflow. We tested the probability of random association between flood years and high streamflow at gauge G814001 using superposed epoch analysis. We found that mean reconstructed flows across these 6 years are significantly higher ($p < 0.01$) than would be expected by chance (Figure 6). The ability of the reconstruction to identify pre-calibration historical flood events increases confidence in the reconstruction model outside of the instrumental period.

4.4. Extreme Events

Surface warming of the equatorial Pacific associated with El Niño events drives an intensification of the Walker circulation, resulting in decreased average deep convection over Australia (Holland, 1988; McBride & Nicholls, 1983). The reverse occurs during La Niña events, with weakening of the Walker Circulation and increased convection. However, this relationship is not symmetric, with La Niña events generally more highly correlated with rainfall over Australia than El Niño events (Power et al., 2006; Risbey et al., 2009). Teleconnections between ENSO phases and Australian rainfall also vary with the phases of the Interdecadal Pacific Oscillation, with warm (positive) phases decreasing the strength and spatial coherence of ENSO-rainfall relationships (Power et al., 1999). Recent research (Allen et al., 2020) has shown that precipitation at the end of the wet season (March–May) in monsoonal Australia is asymmetrically linked to ENSO, with increasingly extreme wet events associated with increasingly cooler SSTs, but less clear relationships between dry extremes and El Niño phases.

We tested the relationship between annual Daly River streamflow extremes and Pacific SSTs by comparing the number of high and low streamflow events that co-occurred with a known ENSO event. Figure 7 shows that

extreme high streamflow events, defined as exceeding the 95th percentile of reconstructed flow, are significantly linked to Pacific SST anomalies, as demonstrated by the significant co-occurrence with La Niña events. Conversely, low flow events, defined as below the 5th percentile of reconstructed flow, were found to significantly *not* co-occur with La Niña events. El Niño events were not found to be significantly related to either high or low flow extremes, with the number of co-occurring events very similar to the mean of the bootstrap distribution. Not all El Niño events are associated with weak IASM rainfall. While lower-than-average monsoon rainfall occurs during canonical El Niño events, there is little change in total rainfall during El Niño Modoki events, which result in a shorter but more intense monsoon (Taschetto et al., 2010). We tested the relationships between El Niño events and Daly River low flow extremes for canonical El Niño and El Niño Modoki events separately, but again the results were not significant (Figure S11 in Supporting Information S1).

These findings are consistent with the relationship between cool Pacific SSTs and rainfall over Australia in observations, and are similar to the findings of Allen et al. (2020), despite the differences in the study season. Figure 7, panels (e) and (f), shows the composite December–January SSTs over the 9 extreme low and 15 extreme high flow years. High streamflow years are associated with warmer-than-average SSTs off the coast of Australia which lead to greater convection and monsoon rainfall, whereas low flow extremes are associated with cool SST anomalies and suppressed convection (BOM, 2012). The mechanisms behind the asymmetrical relationship between ENSO and northern Australian rainfall and streamflow is an area of active research, with the interaction between ENSO and other modes of variability a likely cause (Cai & van Rensch, 2013; Heidemann et al., 2021; Power et al., 2006).

While high total annual streamflow is more likely to occur during a La Niña than El Niño phase, the rainfall events that cause significant flooding at Katherine cannot be linked to ENSO phasing based on the available data. While the flooding at Katherine during 2011 was associated with a strong La Niña that also caused extensive flooding in Eastern Australia, other major historical floods at Katherine have occurred during years with average Pacific SSTs and El Niño years. As most of the region's rain falls as intense, intermittent, tropical showers, monsoon troughs, or ex-tropical cyclone lows, rain events during average years are sufficient to cause local flooding. Tropical cyclones in the instrumental record are ∼20% more likely to occur in northern Australia during La Niña years (Kuleshov et al., 2009), but ENSO phases do not significantly impact the occurrence of monsoon bursts which are more likely to occur during active phases of the Madden–Julian Oscillation (Berry & Reeder, 2016). Rainfall event timing linked to antecedent conditions is also a factor, with heavy rainfalls occurring later in the wet season when the subsurface is saturated more likely to result in extreme discharge than equivalent events earlier in the season (Chappell & Bardsley, 1985).

Indian Ocean SSTs also affect northern Australian rainfall, with positive phases of the Indian Ocean Dipole (IOD) linked to decreased winter-spring rainfall. The influence of the IOD begins in May–June, and peaks in September–October, diminishing rapidly at the start of the monsoon. Therefore, the IOD has very little impact on the peak of the monsoon (Jourdain et al., 2013; Taschetto et al., 2010), and, as expected, we found no relationship between the IOD and Daly River annual average or extreme streamflow. An IASM-region streamflow reconstruction for the Citarum Basin in Java, Indonesia, which specifically targets spring (Sept-Nov) streamflow, has shown an increase in the frequency of low streamflow events accompanying the increase in the frequency and magnitude of positive IOD events since the 1960s (D'Arrigo et al., 2011). This illustrates the importance of the seasonality of reconstructions when considering the impacts of different climate drivers on extreme events in the IASM region.

Changes in the frequency of extreme low and high streamflow events in the Daly catchment were investigated using a Gaussian kernel technique. Results for the Katherine River and Daly River gauge G8140040 are shown in Figures 8a and 8b and remaining gauges in Figure S12 in Supporting Information S1. Persistent weak monsoons have been proposed as the cause of the sixteenth-century megadrought (1560–1587 CE) in monsoon Asia (Cook et al., 2010). We also see a peak in the occurrence of low flow events in the mid-sixteenth century, noting that the Daly River reconstruction is not independent of the drought reconstruction of Cook et al. (2010).

The mid-1600s to early 1800s shows low reconstruction variance and a low frequency of both low and high streamflow events. Paleoclimate studies suggest two potential mechanisms that could explain this result. The low variance period broadly coincides with the Little Ice Age (LIA), a period of lower-than-average temperatures in the Northern Hemisphere, believed to result from both low solar activity (Maunder and Dalton grand solar minima) and high volcanic activity (Grove, 1988). Climate proxy reconstructions and modeling suggest

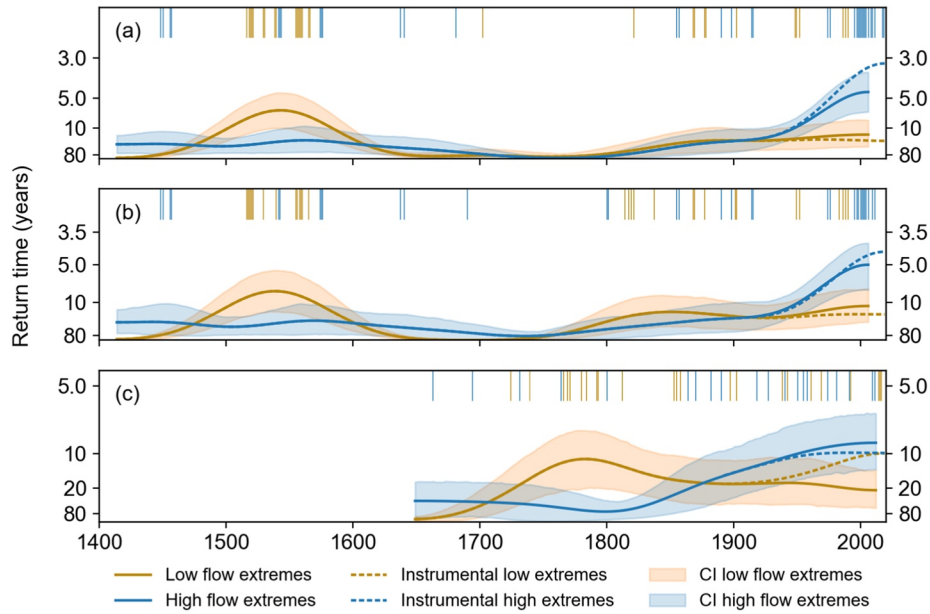

Figure 8. Extreme high flow/low flow event years and the time-varying frequency of the occurrence of these events between 1413 and 2018 for the (a) Daly River at G8140040 and (b) Katherine River at G8140001. A kernel smoothing method was used with a bandwidth of 38 years (solid lines), with dashed lines showing the adjusted frequency curve if instrumental data is appended to the reconstruction after 2005. In (c), the frequency of extremes between 1648 and 2018 for the Burdekin River coral reconstruction of Lough (2015) is plotted with a bandwidth of 38 years, with instrumental data appended to the reconstruction after 2011. The shaded areas (blue and orange) represent the 95% confidence intervals based on 1,000 bootstrap simulations.

a contraction of the seasonal latitudinal migration of the Intertropical Convergence Zone (ITCZ) during the LIA, with modest rainfall reductions over monsoonal Australia, centered on the 1600–1700 CE period (Denniston et al., 2016; Yan et al., 2015). Proxy reconstructions of ENSO by D'Arrigo et al. (2005) and McGregor et al. (2010) have also identified a period of low ENSO amplitude over the 17th and 18th centuries, although their findings disagree with other studies (Cobb et al., 2003). Either smaller north-south movements of the ITCZ or lower ENSO amplitude could plausibly result in lower monsoon streamflow variability during the LIA.

Figure 8 shows that the occurrence of high flow events has increased markedly over the last ~100 years. A significant ($p < 0.001$) increasing trend in 95th and 90th percentile flows at Daly River gauge G8140040 was identified over the period 1800 to 2018 CE using the Cox-Lewis test against the null hypothesis of a constant occurrence rate. Noting that the Daly catchment gauge reconstructions are not independent, trends in both 95th and 90th percentile flows at Katherine River gauge G8140001 were also significant over this interval ($p < 0.01$; $p = 0.05$, respectively), although the increase in high flows began slightly earlier at ~1770 CE. The results did not change if either the reconstruction end date of 2005 or the observation end date of 2018 were used, and increasing trends calculated over the entire reconstruction interval from 1413 CE were also significant for both gauges.

A sand splay deposit taken at the Nancar Hideout on the lower Daly River, close to the location of streamflow gauge G8140040, shows that low rates of deposition occurred from ~1420 to ~1760 CE, indicating a dry period, followed by an increase in deposition and streamflow in the period from ~1760 to 2005 CE (Wasson et al., 2010). Flood frequency derived from the sediment cores has risen steadily over the last ~160 years, with a doubling in the last ~60 years (Wasson et al., 2010). Noting the dating uncertainties (±10–60 years), this record is highly consistent with our tree ring-based reconstruction, providing independent verification of the recent trend in extreme streamflow.

4.5. Regional Coherency

To test whether recent increases in monsoon streamflow are regionally coherent or unique to the Daly catchment, we compared our terrestrial proxy reconstruction to a coral luminescence-based reconstruction of the Burdekin

River from 1648 to 2011 (Lough et al., 2015). The Burdekin River, located in the dry tropics of Northeast Queensland (Figure 1), also experiences wet season rainfall related to the IASM. Lough et al. (2015) found an increase in the magnitude and frequency of high flow events from the mid-1900s compared to the preceding century in their Burdekin streamflow reconstruction.

We assessed changes in Burdekin River streamflow using the same methods described above for the Daly catchment (Figure 8c), extending the reconstruction from 2011 to 2018 using instrumental data. As for the Daly catchment, trends in both 95th and 90th percentile Burdekin River flows increased significantly over the interval from 1800 to 2018 CE ($p < 0.05$), with trends also significant since the beginning of the reconstruction period at 1648 CE ($p < 0.05$).

Both catchment and rainfall changes may have contributed to the increasing streamflow trends. Agricultural development in the Burdekin Catchment since the settlement period (1851–1900) has likely contributed to higher discharge through vegetation cover and soil compaction changes to rainfall-runoff ratios (Lough et al., 2015). However, there are currently low levels of development and intensive agriculture in the Daly, with less than 10% of land under intensive use (Álvarez-Romero et al., 2016). Land surface changes, therefore, are unlikely to have had a significant contribution to the observed increase in streamflow in the Daly River or the coherent trend between the catchments.

Recent increasing trends in northern Australia summer rainfall are well documented. The increasing trend has been observed using rainfall data from 1900 onward, but may have begun in the early 1800s (Gallego et al., 2017). The trend has intensified since the 1950s (Nicholls, 2004; Rotstayn et al., 2007; Suppiah, 1992; Taschetto & England, 2009), which matches the observed changes in the frequency of extreme events in the Daly and Burdekin catchments. Most of the increasing rainfall trend can be explained by an increase in the frequency of multi-day rainfall events during active monsoon phases, rather than changes in the intensity of individual rainfall events (Clark et al., 2018; Dey et al., 2020). This implies that the weather systems causing heavy rainfall patterns are developing more often (Clark et al., 2018).

The mechanisms behind increasing monsoon rainfall are still unclear. Recent changes in ENSO are not a contributing factor as the increased frequency of El Niño events in the late twentieth Century should result in fewer wet years and fewer high annual streamflow events (Shi et al., 2008). Nor does the trend follow the thermodynamic increase in rainfall event intensity expected with climate change (Berry et al., 2011; Clark et al., 2018; Smith et al., 2008). Rotstayn et al. (2007) showed that increased concentrations of anthropogenic aerosols can drive temperature and pressure-induced changes in monsoonal winds and increased precipitation in climate modeling, but these findings were later disputed (Shi et al., 2008). Changes in regional sea surface temperatures (Shi et al., 2008), land-ocean temperature differences (Wardle & Smith, 2004), and timing of the monsoon onset (Taschetto & England, 2009), are also proposed mechanisms. It follows that the causes of the recent increasing trend in Daly and Burdekin annual streamflow totals are currently unknown, and further research effort is required.

5. Conclusions

A long-term perspective on past northern Australian streamflow variability is provided by our tree-ring reconstruction for the Daly catchment, one of the few high-resolution streamflow proxy reconstructions for the IASM region. Despite the relatively short length of the instrumental records used for calibration and verification, little decrease in model statistics was observed moving back in time, indicating that the reconstruction provides useful information throughout the reconstruction period. Our Daly catchment reconstruction extends the record by more than five centuries. The length and robustness of the reconstruction, ability to identify historical flood events and coherence with other proxy reconstructions demonstrate the utility of the variance transform methodology to isolate streamflow signals from noisy tree-ring proxies, particularly when proxies far from the reconstruction target location are used. This method can be applied to reconstructions from other catchments in regions with few local proxies.

The reconstruction shows that high annual streamflow in the Daly catchment is associated with La Niña events, but low streamflow is not associated with El Niño events, confirming previous findings that IASM rainfall

responds asymmetrically to ENSO. More generally, warm (cool) SST anomalies near the Australian coastline are associated with high (low) annual streamflow due to enhanced (suppressed) convection.

The recent magnitude and frequency of high streamflow events is unmatched over the past five centuries, regionally coherent, and closely follows observed trends in summer monsoon rainfall. The mechanisms behind the increasing trend in monsoon rainfall, and thus streamflow, are currently unknown. Increasing annual streamflow cannot be directly interpreted as a trend in flood hazard, because the increased frequency of rainfall events rather than increased event intensity lies behind this trend. The short duration high-intensity rainfall events that cause flooding at Katherine can occur in otherwise dry years, and antecedent catchment conditions and tropical cyclone events also contribute to flood occurrence.

Although it is unclear how average IASM rainfall will change with continued global warming, rainfall variability will likely increase. The consecutive failure of two monsoon seasons in 2019 and 2020 demonstrate that despite robust and regionally coherent trends in high streamflow, multi-year dry events still occur. Increased variability could have serious implications for water resources in the Daly catchment, as ecological and social functions rely on dry season baseflow from aquifers recharged during the previous summer's monsoon. Our reconstruction shows that current resource allocations in the Daly have been set during a period of unprecedented high river and aquifer levels which should be carefully considered by water managers when deciding on sustainable future allocations

Conflict of Interest

The authors declare no conflicts of interest relevant to this study.

Data Availability Statement

All tree-ring chronologies included in the modelling are publicly available from the NOAA/World Data Service for Paleoclimatology archives at https://www.ncdc.noaa.gov. The code underpinning this paper is available on request from the corresponding author.

Acknowledgments
The authors acknowledge the efforts of all the dendrochronologists who have contributed tree-ring chronologies to the ITRDB, allowing for studies such as this one to be undertaken. Our thanks also to Ze Jiang for his helpful discussions on methodology and to Hung Nguyen and two anonymous reviewers, whose comments have improved this manuscript. PAH is supported by an Australian Government Research Training Scholarship and the UNSW Scientia PhD Scholarship Scheme. MPR is supported by a NOAA Climate and Global Change Fellowship under UCAR CPAESS award #NA18NWS4620043B. FJ is supported by the UNSW Scientia Program. Further support provided by the ARC Centre of Excellence in Australian Biodiversity and Heritage (CE170100015). Open access publishing facilitated by University of New South Wales, as part of the Wiley - University of New South Wales agreement via the Council of Australian University Librarians.

References

Adler, R. F., Huffman, G. J., Chang, A., Ferraro, R., Xie, P. P., Janowiak, J., et al. (2003). The Version-2 Global Precipitation Climatology Project (GPCP) Monthly Precipitation Analysis (1979-present). *Journal of Hydrometeorology*, *4*(6), 1147–1167. https://doi.org/10.1175/1525-7541(2003)004<1147:TVGPCP>2.0.CO;2

Allen, K. J., Brookhouse, M., French, B. J., Nichols, S. C., Dahl, B., Norrie, D., et al. (2019). Two climate-sensitive tree-ring chronologies from Arnhem Land, monsoonal Australia. *Austral Ecology*, *44*(4), 581–596. https://doi.org/10.1111/aec.12699

Allen, K. J., Freund, M. B., Palmer, J. G., Simkin, R., Williams, L., Brookhouse, M., et al. (2020). Hydroclimate extremes in a north Australian drought reconstruction asymmetrically linked with Central Pacific Sea surface temperatures. *Global and Planetary Change*, *195*(July), 103329. https://doi.org/10.1016/j.gloplacha.2020.103329

Allen, K. J., Lee, G., Ling, F., Allie, S., Willis, M., & Baker, P. J. (2015). Palaeohydrology in climatological context: Developing the case for use of remote predictors in Australian streamflow reconstructions. *Applied Geography*, *64*, 132–152. https://doi.org/10.1016/j.apgeog.2015.09.007

Álvarez-Romero, J., Adams, V., & Pressey, R. (2016). Using optimal land-use scenarios to assess trade-offs between conservation, development, and social values. *PLoS One*, *11*(6), e0158350. https://doi.org/10.1371/journal.pone.0158350

Baker, P. J., Palmer, J. G., & D'Arrigo, R. (2008). The dendrochronology of Callitris intratropica in northern Australia: Annual ring structure, chronology development and climate correlations. *Australian Journal of Botany*, *56*(4), 311–320. https://doi.org/10.1071/BT08040

Berry, G., & Reeder, M. (2016). The dynamics of Australian monsoon bursts. *Journal of the Atmospheric Sciences*, *73*(1), 55–69. https://doi.org/10.1175/JAS-D-15-0071.1

Berry, G., Reeder, M. J., & Jakob, C. (2011). Physical mechanisms regulating summertime rainfall over Northwestern Australia. *Journal of Climate*, *24*(14), 3705–3717. https://doi.org/10.1175/2011JCLI3943.1

BOM (2012). *Record-breaking La Niña events. An analysis of the La Niña life cycle and the impacts and significance of the 2010–11 and 2011–12 La Niña events in Australia*. Retrieved from http://www.bom.gov.au/climate/enso/history/La-Nina-2010-12.pdf

BOM (2019). Climate of the 2018–19 financial year. In *Australian Government Bureau of Meteorology Climate Updates*. Retrieved from http://www.bom.gov.au/climate/updates/articles/a034.shtml

BOM (2020). Climate of the 2019–20 financial year. In *Australian Government Bureau of Meteorology Climate Updates*. Retrieved from http://www.bom.gov.au/climate/updates/articles/a037.shtml

Briffa, K. R., Jones, P. D., Bartholin, T. S., Eckstein, D., Schweingruber, F. H., Karlén, W., et al. (1992). Fennoscandian summers from AD 500: Temperature changes on short and long timescales. *Climate Dynamics*, *7*(3), 111–119. https://doi.org/10.1007/BF00211153

Brown, J. R., Moise, A. F., & Colman, R. A. (2017). Projected increases in daily to decadal variability of Asian-Australian monsoon rainfall. *Geophysical Research Letters*, *44*(11), 5683–5690. https://doi.org/10.1002/2017GL073217

Cai, W., & Renschvan, P. (2013). Austral summer teleconnections of Indo-Pacific variability: Their nonlinearity and impacts on Australian climate. *Journal of Climate*, *26*(9), 2796–2810. https://doi.org/10.1175/JCLI-D-12-00458.1

Chappell, J., & Bardsley, K. (1985). *Hydrology of the lower Daly River, Northern Territory*. Australian National University North Australia Research Unit.

Christensen, J. H., Krishna Kumar, K., Aldrian, E., An, S.-I., Cavalcanti, I. F. A., Castrode, M., et al. (2013). Climate phenomena and their relevance for future regional climate change. In V.B., T. F.Stocker, D.Qin, G.-K.Plattner, M.Tignor, S. K.Allen, J.Boschung, A.Nauels, Y.Xia, & P. M.Midgley (Eds.), *Climate change 2013: The physical science basis. Contribution of working Group I to the fifth assessment report of the intergovernmental panel on climate change*. Cambridge University Press.

Clark, S., Reeder, M. J., & Jakob, C. (2018). Rainfall regimes over northwestern Australia. *Quarterly Journal of the Royal Meteorological Society*, *144*(711), 458–467. https://doi.org/10.1002/qj.3217

Cobb, K. M., Charles, C. D., Cheng, H., & Edwards, R. L. (2003). El Niño/Southern Oscillation and tropical Pacific climate during the last millennium. *Nature*, *424*(6946), 271–276. https://doi.org/10.1038/nature01779

Cook, E. R. & Kairiukstis, L. A. (Eds.) (1990). *Methods of dendrochronology: applications in the environmental sciences*. Kluwer Academic Publishers. https://doi.org/10.2307/1551446

Cook, E. R., Anchukaitis, K. J., Buckley, B. M., D'Arrigo, R. D., Jacoby, G. C., & Wright, W. E. (2010). Asian monsoon failure and megadrought during the last millennium. *Science*, *328*, 486–489. https://doi.org/10.1126/science.1185188

Cox, D. R., & Lewis, P. A. W. (1966). *The statistical analysis of series of events*. Methuen.

CSIRO. (2009). *Water in the Daly region in Water in the Timor Sea Drainage Division. A report to the Australian Government from the CSIRO Northern Australia Sustainable Yields Project*. pp. 273–361. CSIRO Water for a Healthy Country Flagship.

D'Arrigo, R., Abram, N., Ummenhofer, C., Palmer, J., & Mudelsee, M. (2011). Reconstructed streamflow for Citarum River, Java, Indonesia: Linkages to tropical climate dynamics. *Climate Dynamics*, *36*(3), 451–462. https://doi.org/10.1007/s00382-009-0717-2

D'Arrigo, R., Baker, P., Palmer, J., Anchukaitis, K., & Cook, G. (2008). Experimental reconstruction of monsoon drought variability for Australasia using tree rings and corals. *Geophysical Research Letters*, *35*(12), 1. https://doi.org/10.1029/2008GL034393

D'Arrigo, R., Cook, E. R., Wilson, R. J., Allan, R., & Mann, M. E. (2005). On the variability of ENSO over the past six centuries. *Geophysical Research Letters*, *32*(3), 1–4. https://doi.org/10.1029/2004GL022055

De Loe, R. C., & Kreutzwiser, R. D. (2000). Climate variability, climate change and water resource management in the Great Lakes. *Climatic Change*, *45*, 163–179. https://doi.org/10.1007/978-94-017-3010-5_9

Denniston, R. F., Ummenhofer, C. C., Wanamaker, A. D., Lachniet, M. S., Villarini, G., Asmerom, Y., et al. (2016). Expansion and contraction of the Indo-Pacific tropical rain belt over the last three millennia. *Scientific Reports*, *6*, 1–9. https://doi.org/10.1038/srep34485

Devineni, N., Lall, U., Pederson, N., & Cook, E. (2013). A tree-ring-based reconstruction of Delaware river basin streamflow using hierarchical Bayesian regression. *Journal of Climate*, *26*(12), 4357–4374. https://doi.org/10.1175/JCLI-D-11-00675.1

Dey, R., Gallant, A. J. E., & Lewis, S. C. (2020). Evidence of a continent-wide shift of episodic rainfall in Australia. *Weather and Climate Extremes*, *29*, 100274. https://doi.org/10.1016/j.wace.2020.100274

Efron, B. (1987). Better bootstrap confidence intervals. *Journal of the American Statistical Association*, *82*(397), 171–185. https://doi.org/10.1080/01621459.1987.10478410

Franke, J., Frank, D., Raible, C. C., Esper, J., & Brönnimann, S. (2013). Spectral biases in tree-ring climate proxies. *Nature Climate Change*, *3*(4), 360–364. https://doi.org/10.1038/nclimate1816

Gallego, D., García-Herrera, R., Peña-Ortiz, C., & Ribera, P. (2017). The steady enhancement of the Australian Summer Monsoon in the last 200 years. *Scientific Reports*, *7*(1), 1–7. https://doi.org/10.1038/s41598-017-16414-1

Gelman, A., Goodrich, B., Gabry, J., & Vehtari, A. (2019). R-squared for Bayesian regression models. *The American Statistician*, *73*(3), 307–309. https://doi.org/10.1080/00031305.2018.1549100

Grove, J. M. (1988). *Little Ice Ages: Ancient and Modern (2nd ed.)*. Routledge. https://doi.org/10.4324/9780203505205

Haurwitz, M. W., & Brier, G. W. (1981). A critique of the superposed epoch analysis method: Its application to solar-weather relations. *Monthly Weather Review*, *109*, 2074–2079. https://doi.org/10.1175/1520-0493(1981)109<2074:acotse>2.0.co;2

Heidemann, H., Ribbe, J., Cowan, T., Henley, B. J., Pudmenzky, C., Stone, R., et al. (2021). The influence of interannual and decadal Indo-Pacific sea surface temperature variability on Australian monsoon rainfall. *Journal of Climate*, *35*, 1–444. https://doi.org/10.1175/jcli-d-21-0264.1

Holland, G. J. (1988). Interannual variability of the Australian summer monsoon at Darwin: 1952–82. *Monthly Weather Review*, *114*, 594–604.

Huang, B., Thorne, P. W., Banzon, V. F., Boyer, T., Chepurin, G., Lawrimore, J. H., et al. (2017). Extended reconstructed Sea surface temperature, Version 5 (ERSSTv5): Upgrades, validations, and intercomparisons. *Journal of Climate*, *30*(20), 8179–8205. https://doi.org/10.1175/JCLI-D-16-0836.1

Jiang, Z., Rashid, M. M., Johnson, F., & Sharma, A. (2021). A wavelet-based tool to modulate variance in predictors: An application to predicting drought anomalies. *Environmental Modelling & Software*, *135*, 104907. https://doi.org/10.1016/j.envsoft.2020.104907

Jiang, Z., Sharma, A., & Johnson, F. (2020). Refining predictor spectral representation using wavelet theory for improved natural system modeling. *Water Resources Research*, *53*(3), 1–17. https://doi.org/10.1029/2019WR026962

Jourdain, N. C., Gupta, A. S., Taschetto, A. S., Ummenhofer, C. C., Moise, A. F., & Ashok, K. (2013). The Indo-Australian monsoon and its relationship to ENSO and IOD in reanalysis data and the CMIP3/CMIP5 simulations. *Climate Dynamics*, *41*(11–12), 3073–3102. https://doi.org/10.1007/s00382-013-1676-1

Kuleshov, Y., Ming, F. C., Qi, L., Chouaibou, I., Hoareau, C., & Roux, F. (2009). Tropical cyclone genesis in the Southern Hemisphere and its relationship with the ENSO. *Annales Geophysicae*, *27*(6), 2523–2538. https://doi.org/10.5194/angeo-27-2523-2009

Lough, J. M., Lewis, S. E., & Cantin, N. E. (2015). Freshwater impacts in the central great Barrier Reef: 1648–2011. *Coral Reefs*, *34*(3), 739–751. https://doi.org/10.1007/s00338-015-1297-8

McBride, J. L., & Nicholls, N. (1983). Seasonal relationships between Australian rainfall and the southern oscillation. *Monthly Weather Review*, *111*, 1998–2004. https://doi.org/10.1175/1520-0493(1983)111<1998:srbara>2.0.co;2

McCallum, J. L., Crosbie, R. S., Walker, G. R., & Dawes, W. R. (2010). Impacts of climate change on groundwater in Australia: A sensitivity analysis of recharge. *Hydrogeology Journal*, *18*(7), 1625–1638. https://doi.org/10.1007/s10040-010-0624-y

McGregor, S., Timmermann, A., & Timm, O. (2010). A unified proxy for ENSO and PDO variability since 1650. *Climate of the Past*, *6*(1), 1–17. https://doi.org/10.5194/cp-6-1-2010

Meko, D., Stockton, C. W., & Boggess, W. R. (1995). The tree-ring record of severe sustained drought. *JAWRA Journal of the American Water Resources Association*, *31*(5), 789–801. https://doi.org/10.1111/j.1752-1688.1995.tb03401.x

Melvin, T. M., & Briffa, K. R. (2008). A "signal-free" approach to dendroclimatic standardisation. *Dendrochronologia*, *26*(2), 71–86. https://doi.org/10.1016/j.dendro.2007.12.001

Morrison, R. E. (1970). *Water resources of the Daly River Basin - A study of a proposed dam at Mt. Nancar. Masters of Engineering Science in Water Engineering*. The University of New South Wales.

Mudelsee, M., Börngen, M., Tetzlaff, G., & Grünewald, U. (2003). No upward trends in the occurrence of extreme floods in central Europe. *Nature*, *425*(6954), 166–169. https://doi.org/10.1038/nature01928

Mudelsee, M., Börngen, M., Tetzlaff, G., & Grünewald, U. (2004). Extreme floods in central Europe over the past 500 years: Role of cyclone pathway "Zugstrasse Vb." *Journal of Geophysical Research - D: Atmospheres*, *109*(23), 1–21. https://doi.org/10.1029/2004JD005034

Nash, J. E., & Sutcliffe, J. V. (1970). River flow forecasting through conceptual model. Part 1—A discussion of principles. *Journal of Hydrology*, *10*, 282–290. https://doi.org/10.1016/0022-1694(70)90255-6

Nguyen, H. T. T., Turner, S. W. D., Buckley, B. M., & Galelli, S. (2020). Coherent streamflow variability in monsoon Asia over the past eight centuries—Links to oceanic drivers. *Water Resources Research*, *56*(12), 1–20. https://doi.org/10.1029/2020WR027883

Nicholls, N. (2004). The changing nature of Australian droughts. *Climatic Change*, *63*(3), 323–336. https://doi.org/10.1023/B:CLIM.0000018515.46344.6d

O'Donnell, A. J., Cook, E. R., Palmer, J. G., Turney, C. S. M., Page, G. F. M., & Grierson, P. F. (2015). Tree rings show recent high summer-autumn precipitation in northwest Australia is unprecedented within the last two centuries. *PLoS One*, *10*(6), 1–18. https://doi.org/10.1371/journal.pone.0128533

Petheram, C., McMahon, T. A., & Peel, M. C. (2008). Flow characteristics of rivers in northern Australia: Implications for development. *Journal of Hydrology*, *357*(1–2), 93–111. https://doi.org/10.1016/j.jhydrol.2008.05.008

Power, S. B., Casey, T., Folland, C., Colman, A., & Mehta, V. (1999). Inter-decadal modulation of the impact of ENSO on Australia. *Climate Dynamics*, *15*(5), 319–324. https://doi.org/10.1007/s003820050284

Power, S. B., Haylock, M., Colman, R., & Wang, X. (2006). The predictability of interdecadal changes in ENSO activity and ENSO teleconnections. *Journal of Climate*, *19*(19), 4755–4771. https://doi.org/10.1175/JCLI3868.1

Rao, M. P., Cook, E. R., Cook, B. I., Anchukaitis, K. J., D'Arrigo, R. D., Krusic, P. J., et al. (2019). A double bootstrap approach to Superposed Epoch Analysis to evaluate response uncertainty. *Dendrochronologia*, *55*(February), 119–124. https://doi.org/10.1016/j.dendro.2019.05.001

Rao, M. P., Cook, E. R., Cook, B. I., D'Arrigo, R. D., Palmer, J. G., Lall, U., et al. (2020). Seven centuries of reconstructed Brahmaputra River discharge demonstrate underestimated high discharge and flood hazard frequency. *Nature Communications*, *11*(1). https://doi.org/10.1038/s41467-020-19795-6

Rao, M. P., Cook, E. R., Cook, B. I., Palmer, J. G., Uriarte, M., Devineni, N., et al. (2018). Six centuries of Upper Indus basin streamflow variability and its climatic drivers. *Water Resources Research*, *54*(8), 5687–5701. https://doi.org/10.1029/2018WR023080

Rice, J. L., Woodhouse, C. A., & Lukas, J. J. (2009). Science and decision making: Water management and tree-ring data in the western United States. *Journal of the American Water Resources Association*, *45*(5), 1248–1259. https://doi.org/10.1111/j.1752-1688.2009.00358.x

Risbey, J. S., Pook, M. J., McIntosh, P. C., Wheeler, M. C., & Hendon, H. H. (2009). On the remote drivers of rainfall variability in Australia. *Monthly Weather Review*, *137*(10), 3233–3253. https://doi.org/10.1175/2009MWR2861.1

Rotstayn, L. D., Cai, W., Dix, M. R., Farquhar, G. D., Feng, Y., Ginoux, P., et al. (2007). Have Australian rainfall and cloudiness increased due to the remote effects of Asian anthropogenic aerosols? *Journal of Geophysical Research: Atmospheres*, *112*(9), 1–28. https://doi.org/10.1029/2006JD007712

Rozendaal, D. M. A., & Zuidema, P. A. (2011). Dendroecology in the tropics: A review. *Trees - Structure and Function*, *25*(1), 3–16. https://doi.org/10.1007/s00468-010-0480-3

Russell-Smith, J., Lucas, D., Gapindi, M., Gunbunuka, B., Kapirigi, N., Namingum, G., et al. (1997). Aboriginal resource utilization and fire management practice in western Arnhem land, monsoonal northern Australia: Notes for prehistory, lessons for the future. *Human Ecology*, *25*(2), 159–195. https://doi.org/10.1023/a:1021970021670

Sheather, S. J., & Jones, M. C. (1991). A reliable data-based bandwidth selection method for kernel density estimation. *Journal of the Royal Statistical Society*, *53*(3), 683–690. https://doi.org/10.1111/j.2517-6161.1991.tb01857.x

Shi, G., Cai, W., Cowan, T., Ribbe, J., Rotstayn, L., & Dix, M. (2008). Variability and trend of North West Australia rainfall: Observations and coupled climate modeling. *Journal of Climate*, *21*(12), 2938–2959. https://doi.org/10.1175/2007JCLI1908.1

Singh, D., Ghosh, S., Roxy, M. K., & McDermid, S. (2019). Indian summer monsoon: Extreme events, historical changes, and role of anthropogenic forcings. *Wiley Interdisciplinary Reviews: Climate Change*, *10*(2), 1–35. https://doi.org/10.1002/wcc.571

Skertchly, A., & Skertchly, K. (1999). The Katherine-Daly flood disaster 1998. *Australian Journal of Emergency Management*, 14(1), 31–36.

Smith, I. N., Wilson, L., & Suppiah, R. (2008). Characteristics of the northern Australian rainy season. *Journal of Climate*, *21*(17), 4298–4311. https://doi.org/10.1175/2008JCLI2109.1

Suppiah, R. (1992). The Australian summer monsoon: a review. *Progress in Physical Geography*, *16*(3), 283–318. https://doi.org/10.1177/030913339201600302

Taschetto, A. S., & England, M. H. (2009). An analysis of late twentieth century trends in Australian rainfall. *International Journal of Climatology*, *29*, 791–807. https://doi.org/10.1002/joc.1736

Taschetto, A. S., Haarsma, R. J., Sen Gupta, A., Ummenhofer, C. C., & England, M. H. (2010). Teleconnections associated with the intensification of the Australian monsoon during El Niño Modoki events. *IOP Conference Series: Earth and Environmental Science*, *11*, 012031. https://doi.org/10.1088/1755-1315/11/1/012031

Verdon-Kidd, D. C., Hancock, G. R., & Lowry, J. B. (2017). A 507-year rainfall and runoff reconstruction for the Monsoonal North West, Australia derived from remote paleoclimate archives. *Global and Planetary Change*, *158*(September), 21–35. https://doi.org/10.1016/j.gloplacha.2017.09.003

Wang, P. X., Wang, B., Cheng, H., Fasullo, J., Guo, Z. T., Kiefer, T., et al. (2014). The global monsoon across timescales: Coherent variability of regional monsoons. *Climate of the Past*, *10*(6), 2007–2052. https://doi.org/10.5194/cp-10-2007-2014

Wardle, R., & Smith, I. (2004). Modeled response of the Australian monsoon to changes in land surface temperatures. *Geophysical Research Letters*, *31*(16). https://doi.org/10.1029/2004GL020157

Wasko, C., Shao, Y., Vogel, E., Wilson, L., Wang, Q. J., Frost, A., & Donnelly, C. (2021). Understanding trends in hydrologic extremes across Australia. *Journal of Hydrology*, *593*, 125877. https://doi.org/10.1016/j.jhydrol.2020.125877

Wasson, R. J., Furlonger, L., Parry, D., Pietsch, T., Valentine, E., & Williams, D. (2010). Sediment sources and channel dynamics, Daly River, northern Australia. *Geomorphology*, *114*(3), 161–174. https://doi.org/10.1016/j.geomorph.2009.06.022

Water Studies Pty Ltd. (2000). *Katherine River flood study* (Report No. 02/2000D). NT Department of Lands, Planning and the Environment.

Yan, H., Wei, W., Soon, W., An, Z., Zhou, W., Liu, Z., et al. (2015). Dynamics of the Intertropical Convergence Zone over the western Pacific during the Little Ice Age. *Nature Geoscience*, *8*(4), 315–320. https://doi.org/10.1038/ngeo2375

Yeates, S. J., Strickland, G. R., & Grundy, P. R. (2013). Can sustainable cotton production systems be developed for tropical northern Australia? *Crop and Pasture Science*, *64*, 1127–1140. https://doi.org/10.1071/CP13220

Zhang, X. S., Amirthanathan, G. E., Bari, M. A., Laugesen, R. M., Shin, D., Kent, D. M., et al. (2016). How streamflow has changed across Australia since the 1950s: Evidence from the network of hydrologic reference stations. *Hydrology and Earth System Sciences*, *20*(9), 3947–3965. https://doi.org/10.5194/hess-20-3947-2016

References From the Supporting Information

Adams, J. B., Mann, M. E., & Ammann, C. M. (2003). Proxy evidence for an El Niño-like response to volcanic forcing. *Nature*, *426*, 274–278. https://doi.org/10.1038/nature02101

Artigue, H., & Smith, G. (2019). The principal problem with principal components regression. *Cogent Mathematics & Statistics*, *6*(1), 2574–2558. https://doi.org/10.1080/25742558.2019.1622190

Briffa, K. R., Jones, P. D., Pilcher, J. R., & Hughes, M. K. (1988). Reconstructing summer temperatures in northern Fennoscandinavia back to AD 1700 using tree-ring data from Scots pine. *Arctic & Alpine Research*, *20*(4), 385–394. https://doi.org/10.2307/1551336

Freund, M. B., Henley, B. J., Karoly, D. J., McGregor, H. V., Abram, N. J., & Dommenget, D. (2019). Higher frequency of Central Pacific El Niño events in recent decades relative to past centuries. *Nature Geoscience*, *12*(6), 450–455. https://doi.org/10.1038/s41561-019-0353-3

Gelman, A., & Hill, J. (2006). *Applied regression and multilevel/hierarchical models*. Cambridge University Press.

Hadi, A. S., & Ling, R. F. (1998). Some cautionary notes on the use of principal components regression. *The American Statistician*, *52*(1), 15–19. https://doi.org/10.1080/00031305.1998.10480530

Higgins, P. A., Palmer, J. G., Turney, C. S. M., Andersen, M. S., & Cook, E. R. (2020). One thousand three hundred years of variability in the position of the South Pacific Convergence Zone. *Geophysical Research Letters*, *47*(17), 1–11. https://doi.org/10.1029/2020GL088238

Mosteller, F., & Tukey, J. W. (1977). Data analysis and regression. A second course in statistics. In *Addison-Wesley Series in Behavioral Science: Quantitative Methods*. Retrieved from https://ui.adsabs.harvard.edu/abs/1977dars.book

Palmer, J. G., Cook, E. R., Turney, C. S. M., Allen, K., Fenwick, P., Cook, B. I., et al. (2015). Drought variability in the eastern Australia and New Zealand summer drought atlas (ANZDA, CE 1500-2012) modulated by the Interdecadal Pacific Oscillation. *Environmental Research Letters*, *10*(12). https://doi.org/10.1088/1748-9326/10/12/124002

Sharma, A., & Mehrotra, R. (2014). An information theoretic alternative to model a natural system using observational information alone. *Water Resources Research*, *50*(1), 650–660. https://doi.org/10.1002/2013WR013845

Sharma, A., Mehrotra, R., Li, J., & Jha, S. (2016). A programming tool for nonparametric system prediction using Partial Informational Correlation and Partial Weights. *Environmental Modelling & Software*, *83*, 271–275. https://doi.org/10.1016/j.envsoft.2016.05.021